Elimination of Eddy Current Artifacts in Diffusion-Weighted Echo-Planar Images: The Use of Bipolar Gradients

Andrew L. Alexander, Jay S. Tsuruda, Dennis L. Parker

Small gradient fields resulting from incompletely canceled eddy currents can cause geometric distortion in echo-planar images. Although this distortion is negligible in most echo-planar applications, the large gradient pulses used in diffusion-weighted echo-planar imaging can result in significant image distortion. In this report, it is shown that this distortion can be significantly reduced by the application of bipolar gradient waveforms. Both bipolar diffusion-sensitizing gradients and an inverted gradient preparatory pulse were examined for minimizing the eddy currents responsible for these distortions.

Key words: magnetic resonance imaging; diffusion; echo planar; distortion correction.

INTRODUCTION

Diffusion-weighted (DW) imaging has recently shown significant clinical utility in the diagnosis and management of acute stroke (1–3), diseases related to myelination of white matter (4–6), and characterization of brain tumors (7, 8). Conventional spin-echo DW imaging techniques are highly sensitive to patient motion, which leads to artifacts in the reconstructed images. Single-shot DW echo-planar imaging (EPI) is nearly insensitive to patient motion and, therefore, is very promising for mapping diffusion coefficients in the brain. Calculated image maps of the trace of the apparent diffusion coefficient, diffusion anisotropy, or the full diffusion tensor require the acquisition of several images with different degrees and orientations of diffusion weighting (4, 5). Obviously, any misregistration between images due to motion or image distortion will lead to inaccuracies in the calculations.

Many new clinical MRI systems are equipped with imaging gradients that can achieve relatively large gradient amplitudes (e.g., 23 mT/m on our system) and fast slew rates (e.g., 120 mT/m/ms). These high-performance gradients are capable of much greater diffusion weighting at reduced echo times, thereby improving the signal-to-noise ratios of the diffusion measurements and image quality. Unfortunately, these increased gradient amplitudes and slew rates also induce significant eddy currents, which, if not properly compensated, can result in geometric distortions. Recently, it has been shown that these distortions can be modeled with a simple affine transformation, and then can be corrected retrospectively using an appropriate dewarping on the acquired images (9).

Improvements to eddy current compensation electronics or the pulse sequence gradient waveforms may be able to minimize these distortions and eliminate the need for postprocessing of the distorted images. In this note, we present evidence that the distortion can be almost completely eliminated by the use of bipolar gradient waveforms.

THEORY

Residual gradient fields from eddy currents, which are on during the echo-planar readout, will lead to shifts and distortions in the reconstructed image. These shifts will principally be in the blipped-gradient direction y due to the low image bandwidth in that direction. The direction and amplitude of the residual gradient will determine the type and magnitude of the distortion as predicted by Haselgrove and Moore (9). A residual gradient in the readout (x), blipped-gradient (y) and slice-encode (z) directions will lead to shear, scaling, and translation distortions, respectively, in the y direction.

Eddy currents will be induced whenever a gradient pulse is turned on or off. The eddy currents will be primarily a function of the amplitude of the gradient transition and will be a superposition of multiple exponential decay terms (10, 11). For simplicity, we will examine a single exponential decay with time constant, τ. For a trapezoidal gradient waveform, the rise and fall portions of the diffusion-gradient will induce equal eddy currents, but of opposite sign. The eddy current for a single trapezoidal gradient can be described by

$$J = J_0(e^{-(t-t_a)/\tau} - e^{-(t-t_b)/\tau}) = J_0 e^{-t/\tau}(e^{t_a/\tau} - e^{t_b/\tau}) \quad [1]$$

where t_a and t_b are the times of the rise and fall portions of the trapezoid (refer to first trapezoid in Fig. 1a), t is the time from the initial start of the sequence ($t > t_b > t_a$), and J_0 is the initial eddy current amplitude for each transition. Therefore, for a relatively short trapezoidal pulse, the eddy currents induced by the rising and falling ramps will tend to cancel each other out, which will lead to minimal residual gradients. If, however, the trapezoid is relatively long in duration, such as the case for diffusion gradients, then the eddy currents from the rise and fall ramps of the gradient waveform will not totally cancel, and there will be residual eddy currents after the gradient pulse. The amplitude of the residual eddy cur-

MRM 38:1016–1021 (1997)

From the Department of Radiology, University of Utah, Salt Lake City, Utah 84132.

Address correspondence to: Andrew L. Alexander, Ph.D., AC 213 SOM Medical Imaging Research Lab, Department of Radiology, University of Utah, Salt Lake City, UT 84132.

Received January 30, 1997; revised May 13, 1997; accepted June 2, 1997.

0740-3194/97 $3.00

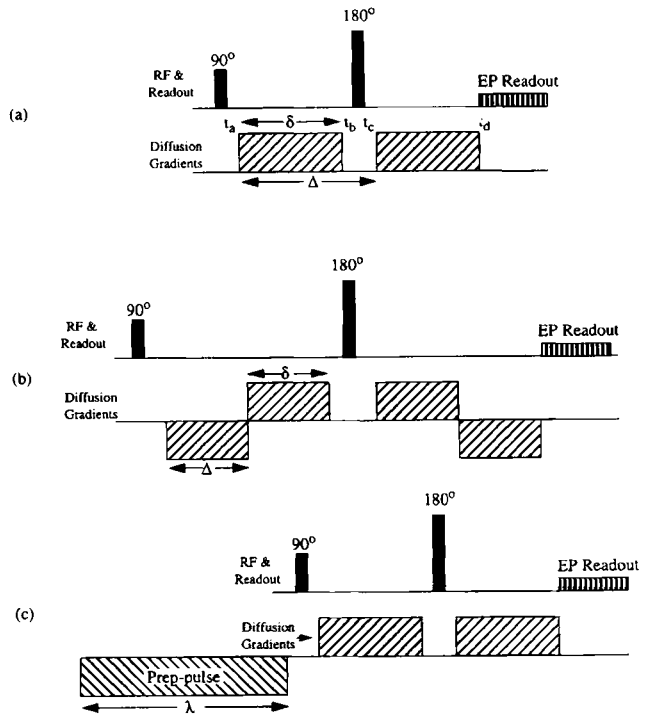

FIG. 1. Schematics of pulse-sequence timing. (a) Standard DW spin-echo EPI sequence (I). (b) Bipolar DW EPI sequence (II). (c) Standard DW EPI sequence (III) with gradient prepulse. Although shown as rectangles, the gradient waveforms are actually trapezoidal with finite ramp widths.

rents will be a function of the pulse amplitude and the pulse duration.

In DW imaging, at least two diffusion gradients are applied. For a pair of diffusion gradients with the same polarity, as shown in Fig. 1a, the residual eddy current after the second diffusion gradient is

$$J = J_0 e^{-t/\tau}[(e^{t_a/\tau} - e^{t_b/\tau}) + (e^{t_c/\tau} - e^{t_d/\tau})] \qquad [2]$$

where t_a and t_d are the start and end times of the second trapezoid. For long eddy current time constants, Eq. [2] can be approximated by the linear relationship,

$$J \approx J_0 e^{-t/\tau}[(t_a - t_b) + (t_c - t_d)]/\tau \qquad [3]$$

If the duration of both diffusion gradients are equal, the residual eddy currents are approximately double that of a single gradient pulse.

Conversely, the eddy currents generated by a pair of diffusion gradients with opposite polarity, as shown in Fig. 1b, will tend to cancel

$$J \approx J_0 e^{-t/\tau}[(t_a - t_b) - (t_c - t_d)]/\tau \approx 0 \qquad [4]$$

If the pulses are otherwise identical, the y distortion will be equal, but in opposite directions. For example, if a positive gradient pulse causes the image to shift by $-y_0$, then a negative gradient pulse will cause the image to shift by $+y_0$.

The timing of a standard DW spin-echo sequence is illustrated in Fig. 1a. One diffusion gradient pulse is applied on each side of the 180° refocusing pulse. For this pulse sequence, the diffusion weighting can be described by

$$S = S_0 e^{-bD} \qquad [5]$$

where S_0 is the signal strength ignoring diffusion, D is the diffusion coefficient, and b is the diffusion weighting factor (12)

$$b = \gamma^2 \int_0^{TE} \left(\int_0^{t'} G(t'')dt'' \right)^2 dt' \qquad [6]$$

Here, γ is the gyromagnetic ratio, $G(t)$ is the gradient waveform, and TE is the echo time. If the diffusion weighting contributions from the imaging gradients are ignored, Eq. [6] and the gradient transition times are short, Eq. [2] becomes

$$b = \gamma^2 G_d^2 \delta^2 \left(\Delta - \frac{\delta}{3} \right) \qquad [7]$$

where G_d is the diffusion gradient amplitude, δ is the width of each diffusion gradient, and Δ is the time difference between the start of the first diffusion gradient and the start of the second. The actual calculation for trapezoidal diffusion gradients was described by Price and Kuchel (13); however, this is a very small correction for the case of relatively short ramp times. In Fig. 1a, both diffusion gradients have the same polarity, and therefore, will have residual eddy currents in the same direction that will add linearly.

Based upon the previous discussion, it would seem that the eddy currents and distortion may be minimized by using more optimal diffusion gradient waveforms. One obvious solution is to use bipolar diffusion gradients on each side of the refocusing pulse as illustrated in Fig. 1b. For bipolar diffusion gradients with no delay between each lobe, Eq. [7] becomes

$$b = \frac{2}{3} \gamma^2 G_d^2 \delta^3 \qquad [8]$$

Since there are two sets of bipolar pulses for the sequence in Fig. 1b, the b value will be twice the result of Eq. [8]. The effective diffusion weighting for two sets of bipolar gradient pulses is less than 25% as efficient as the original unipolar diffusion gradients shown in Fig. 1a. By increasing the duration of the bipolar diffusion gradients in Fig. 1b by 59%, diffusion weighting close to the unipolar case can be achieved. The penalty for doing this is an increase in the minimum echo time. The use of bipolar diffusion gradients for canceling self-induced gradients in DW spin-echo imaging (non-EPI) sequence was described previously by Trudeau *et al.* (14). The minimization of self-induced gradients resulted in more accurate measurements of diffusion anisotropy. This should also be the case for our pulse sequence, in addition to removing the distortion from the EPI readout with the self-induced gradients.

If the time constants for the eddy currents are sufficiently long, the distortion can also be compensated by applying an inverted preparatory gradient pulse before

the initial 90° RF excitation as illustrated in Fig. 1c. This gradient pulse does not contribute to the diffusion weighting, but does generate eddy currents. The amplitude and duration of this gradient should be as least as great as the amplitude and twice the duration of each diffusion gradient. The advantage of this technique is that it does not require an increase in the minimum echo time. Gibbs and Johnson (15) previously implemented and reported using gradient prepulses to cancel the effects of eddy currents in DW NMR spectroscopy. They demonstrated that eddy currents from the diffusion gradients attenuated the NMR peaks, when the gradient prepulses were not used.

METHODS

All imaging was performed at 1.5 Tesla GE SIGNA MRI scanner (General Electric Medical Systems, Milwaukee, WI) with actively shielded gradients using the 5.5 operating system. The gradient system was operated with a maximum strength of 23 mT/m and a slew rate of 120 mT/m/ms on all three axes. EPI images shown in this report were obtained using a quadrature "birdcage" transmit-receive head coil and a DW spin-echo EPI technique.

Our experiments were designed to test two different eddy current compensation schemes to see how well they eliminate the associated distortions. The resultant images will be compared against the conventional unipolar diffusion gradients illustrated in Fig. 1a. The two configurations that were tested include (1) bipolar gradients on each side of the 180° refocusing pulse (Fig. 1b) and (2) inverted gradient prepulse with unipolar diffusion gradients (Fig. 1c). The gradient pulses were trapezoidal with ramp times of 248 μs.

DW brain images of a human volunteer were acquired. The base sequence was a spin echo with a fractional echo-planar readout (76 phase encodes out of 128) to minimize the echo time. The imaging parameters were TR = 1000-ms, 22 × 22-cm^2 field-of-view, 128 × 128 acquisition matrix, a receiver sampling bandwidth of ±84 kHz, and a 7-mm slice thickness. Nine individual images were averaged together to improve the image signal-to-noise ratio. A series of four averaged images was obtained in each case: (1) no diffusion weighting, (2) diffusion weighting in x, (3) diffusion weighting in y, and (4) diffusion weighting in z. For all experiments, the amplitudes of the diffusion gradients and the preparatory pulse was 2.2 G/cm. For each of the three diffusion imaging schemes examined, the diffusion timing parameters, δ and Δ, the prepulse width, λ, the diffusion weighting factor, b, and the echo time, TE, are listed in Table 1. The length, λ, of the preparatory pulse in sequence III was determined empirically, by applying an inverted prepulse without diffusion gradients and trying to match the distortions observed with the unipolar diffusion gradients. A pulse of 120 ms closely matched the distortion of the images in sequence I with the diffusion weighting factors listed in Table 1.

Table 1
Experimental Timing Parameters

Method (sequence)	δ (ms)	Δ (ms)	b (s/mm^2)	TE (ms)	λ (ms)
Unipolar (I)	31	37	893	97	
Bipolar (II)	27	27	905	143	
Unipolar w/prep (III)	31	37	893	97	120

A stroke patient was then imaged with the bipolar gradient sequence (II). Identical imaging parameters to those described for the volunteer were used except TR = 1800 ms and 10 individual images were averaged in each diffusion weighting direction to improve the image quality. Four 7-mm thick slices were imaged in each TR period.

Images of the directional diffusion coefficients, D_{xx}, D_{yy}, and D_{zz}, were estimated from the directional DW images by rewriting Eq. [5] in terms of two DW images for the direction i,

$$D_i = \frac{\ln S_0 - \ln S_i}{b_i - b_0} \qquad [9]$$

where b_i is the diffusion weighting in that direction, S_i is the DW image intensity, b_0 is the diffusion weighting factor with the diffusion gradients set to zero, and S_0 is the image intensity with the diffusion gradients turned off. For simplicity, we do not take into account the diffusion weighting from imaging gradients into our calculations, and assume that b_0 is zero. This will lead to small errors in the true calculation of D. The trace of the diffusion tensor, $\boldsymbol{D}$, was then generated by taking the average of the directional diffusion coefficients,

$$\bar{D} = tr\{\boldsymbol{D}\} = (D_{xx} + D_{yy} + D_{zz})/3 \qquad [10]$$

The degree of diffusion anisotropy was calculated as the root mean square deviation of the directional coefficients from the trace,

$$A_D = \sqrt{\sum_{i=x,y,z} (\bar{D} - D_{ii})^2} \qquad [11]$$

It is obvious that misregistration between DW images will lead to significant errors in the trace and anisotropy image calculations.

RESULTS

A set of images of the volunteer with and without diffusion weighting for the uncompensated (I) sequence are shown in Fig. 2. Diffusion weighting is applied in the x, y, and z directions in parts b, c, and d, respectively. The distortion of these images is obvious. The x diffusion gradient (Fig. 2b) seemed to induce primarily a scaling artifact, whereas the y diffusion gradient (Fig. 2c) caused a shearing artifact. This distortion behavior is indicative of cross-term (x/y) eddy currents in our system. Figures 2e and 2f show the trace and anisotropy images that were obtained from the four raw DW images in (a–d). The effects of the image distortion is especially evident in these composite images. The border of the head in both the trace and anisotropy images is bright and the ana-

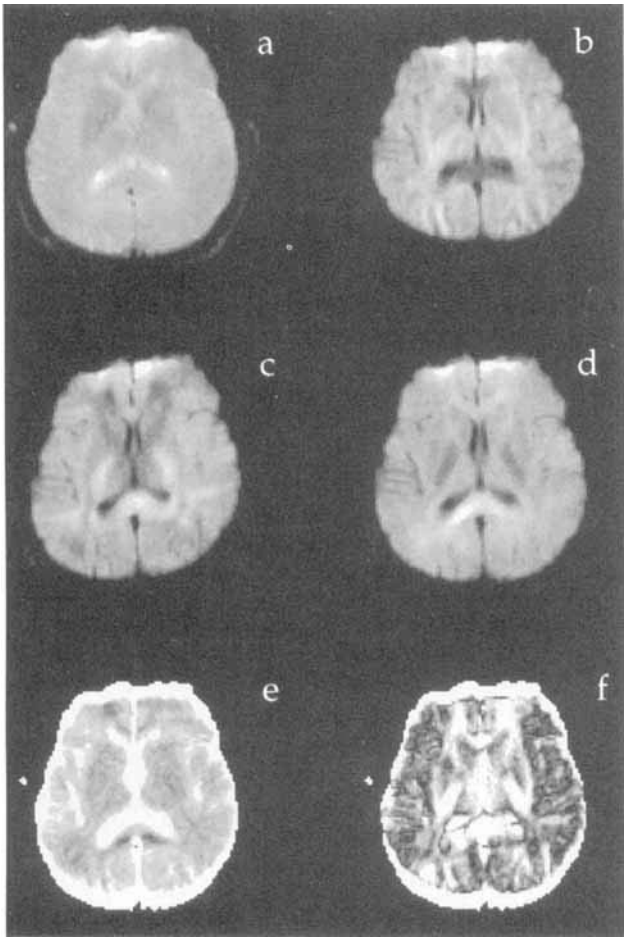

FIG. 2. Average DW images obtained with the standard DW sequence (I): (a) no weighting, (b) *x*, (c) *y*, and (d) *z*. The *x* and *y* DW images demonstrated obvious scaling and shearing distortions, respectively. These images were combined to estimate maps of the (e) diffusion trace and (f) anisotropy. Misregistration of the DW images led to significant errors in the calculated images as is illustrated by the bright bands at the top and bottom periphery of the head.

tomic features seem to be somewhat blurred, which is indicative of the image misregistration. This is consistent with the misregistration artifacts due to eddy currents described by Pierpaoli *et al.* (4).

Bipolar DW images (sequence II) of the same volunteer are shown in Fig. 3. The images do not seem to show any significant distortion. There is no evidence of image misregistration between images in the trace and anisotropy images of Figs. 3e and 3f. Anatomic features appear much sharper in these images than for the uncompensated DW images shown in Fig. 2.

The DW images in Fig. 4 obtained with sequence III demonstrate much less distortion than the uncompensated sequence. The trace and anisotropy images (Figs. 4e and 4f), however, reveal some misregistration, which is indicative that the eddy current correction was not perfect.

The DW images for the 63-year-old male stroke patient at one of the slice locations are shown in Fig. 5. None of the images demonstrated significant distortion due to eddy currents. Each of the averaged raw images (a–d) including the baseline non-DW image, show a region of hyperintense signal indicative of the stroke location. The trace image (Fig. 5e) demonstrated a small drop in the apparent diffusion coefficient of the ischemic region (0.86×10^{-5} cm^2/s) relative to the unaffected brain tissue on the contralateral side (0.99×10^{-5} cm^2/s), which is consistent with the ischemic region being past the hyperacute phase (17–19). Since the drop in the diffusion trace value was relatively small (~14%), the hyperintense signal in Figs. 5a to 5d) is probably due to a result of long T_2. The diffusion in this region appeared to be highly isotropic as indicated by the anisotropy map in Fig. 5f. Conversely, the regional directionality of cerebrospinal fluid flow in the ventricles appears as a high degree of anisotropy in this map. The diffusion images at the other slice locations were similar.

In all images, there is some geometric distortion due to magnetic field inhomogeneities, particularly due to the air within the frontal paranasal sinuses. This distortion was not influenced by either of the eddy current compensation schemes (either II or III).

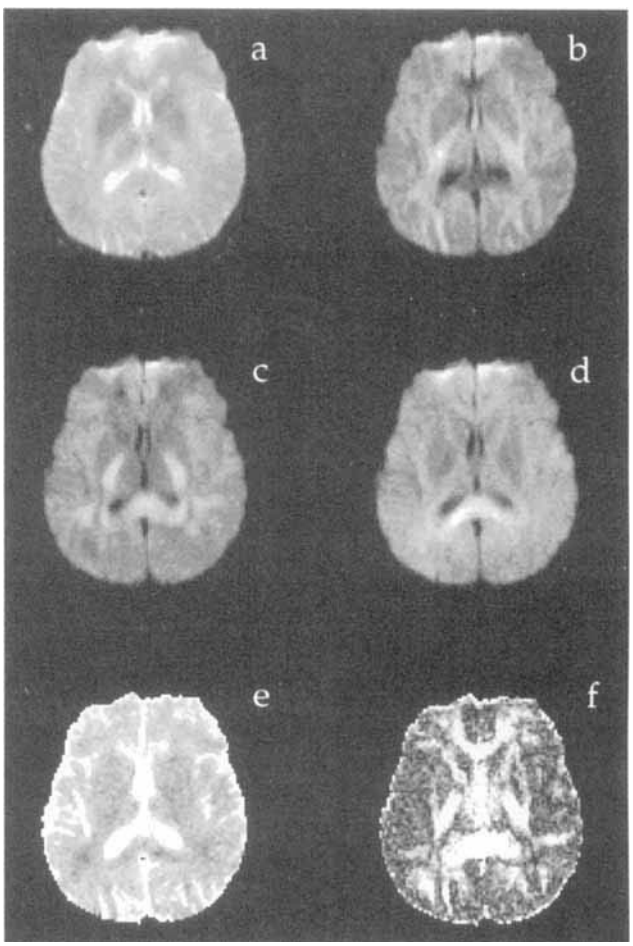

FIG. 3. Average DW images obtained with the bipolar pulse sequence (II): (a) no weighting, (b) *x*, (c) *y*, and (d) *z*. Estimated maps of the diffusion (e) trace and (f) anisotropy are shown. No significant distortion is observed in the average DW images or the calculated images.

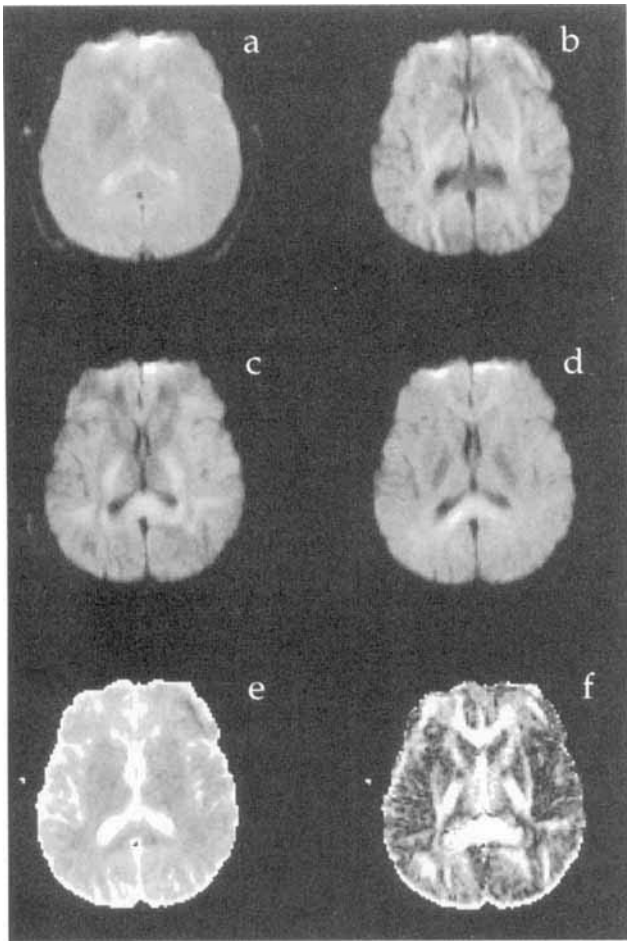

FIG. 4. Average DW images obtained with the pre-pulse sequence (III): (a) no weighting, (b) *x*, (c) *y*, and (d) *z*. Estimated maps of the diffusion (e) trace and (f) anisotropy are shown. The distortion is much less than with the original uncompensated sequence (Fig. 2), but not as good as the bipolar sequence (II) shown in Fig. 3.

DISCUSSION

Both distortion reduction techniques (sequences II and III) seem to significantly reduce the distortion associated with eddy currents due to strong diffusion gradients. Bipolar diffusion gradients seemed to work best, but the prepulse gradient technique may not have been completely optimized for countering the diffusion gradient eddy currents. The time constants of the eddy currents from the prepulse may be too short to effectively cancel the eddy currents from the diffusion gradients. A decrease in either the diffusion gradient amplitudes or echo time may be necessary for full eddy current cancellation. None of these techniques affect the sensitivity of the imaging sequence to patient motion.

The penalty associated with bipolar diffusion gradients (sequence II) is an increase in the echo time. The diminished signal-to-noise ratio, however, is justifiable since the eddy currents and associated distortion have been minimized. Since echo-planar images can be obtained very quickly, a large number of images can be obtained and averaged to improve the signal-to-noise ratio. The diffusion weighting efficiency can also be improved by applying bipolar diffusion gradients on all three axes simultaneously.

The principle advantage of a gradient prepulse (sequence III) is that it does not require an increase in the echo time. Unfortunately, it seems that the prepulse must be larger than both diffusion gradients combined to fully compensate the eddy currents. This will increase the gradient duty cycle and may limit the number of slices that can be interleaved in a single scan. In addition, eddy currents after the prepulse may influence the slice encoding and cause the slice to be either rotated in orientation or scaled in thickness.

The image distortions associated with eddy currents are due to residual gradients that are on during the echo-planar readout. An alternative correction strategy would be to develop an echo-planar readout waveforms that cancel the residual gradient. Calibration of these waveforms is necessary, which may be complicated due to the fact that diffusion gradients in one direction can lead to residual gradients in any direction. The advantage of bipolar diffusion gradients is that no calibration is necessary. It does seem that the gradient prepulse strategy does require calibration, however.

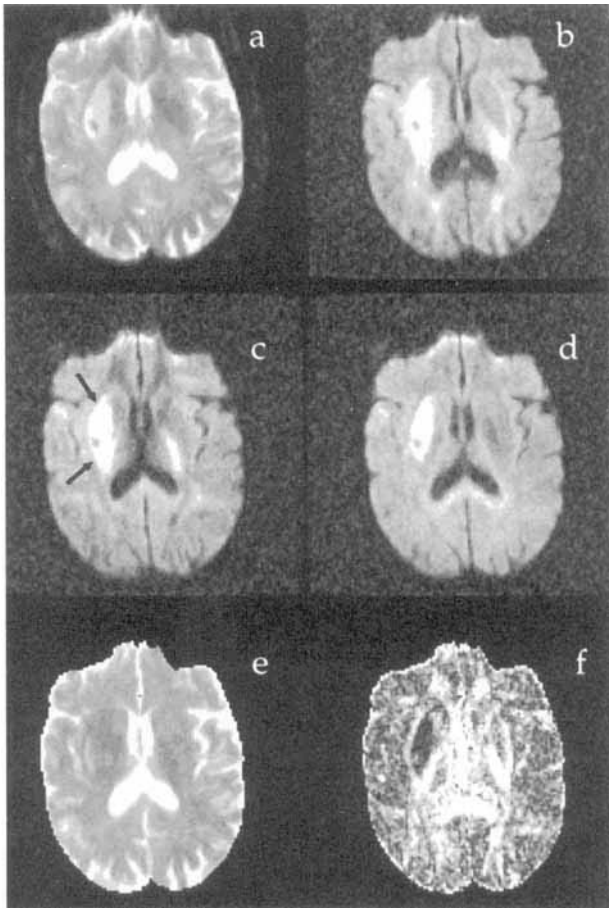

FIG. 5. DW images of a stroke patient acquired using the bipolar sequence (II): (a) no diffusion weighting and diffusion weighting in (b) *x*, (c) *y*, and (d) *z*. The estimated diffusion (e) trace and (f) anisotropy maps are shown. The stroke region is highlighted by an arrow to the hyperintense region in (c).

Eddy currents can also be problematic in other types of DW imaging sequences including turbo-gradient echo (16), spiral scan (20), and radial scan (21) techniques. Bipolar DW techniques should significantly reduce the eddy currents during the readout and improve the image quality for these sequences as well. Conversely, diffusion trace-weighted imaging techniques (22), which implement bipolar diffusion gradients, should inherently be less sensitive to eddy currents.

It should be noted that this technique does not correct for image distortions associated with other sources of magnetic field inhomogeneities from magnetic susceptibilities and poor static field uniformity. These distortions can be quite significant in echo-planar images, which can lead to potential misdiagnoses. These distortions can be minimized by increasing the sampling rates or using multiple-shot EPI techniques. Recently, postprocessing techniques have been described for correcting these distortions by using a measured field map (23).

These results are very promising, yet are still preliminary. Further work needs to be performed to validate these results in general to determine the robustness of the distortion elimination.

CONCLUSION

The results in this study would indicate that it is possible to significantly reduce image distortion due to eddy currents in DW EPI by optimizing the gradient waveforms. Elimination of image distortion is crucial for good image registration between DW images when calculating composite diffusion images, such as the trace, anisotropy, or tensor. The use of bipolar diffusion gradients does not require either calibration of the gradients or postprocessing of the images.

ACKNOWLEDGMENTS

The authors thank for assistance Henry Buswell of the Department of Radiology at the University of Utah, Paul Keller of the Barrow Neurological Institute in Phoenix, AZ, and Ann Shimakawa and Dave Weber of G. E. Medical Systems.

REFERENCES

1. M. Hoehn-Berlage, Diffusion-weighted NMR imaging: application to experimental focal cerebral ischemia. *NMR Biomed.* **7–8,** 345–58 (1995).
2. S. Warach, J. F. Dashe, R. R. Edelman, Clinical outcome in ischemic stroke predicted by early diffusion-weighted and perfusion magnetic resonance imaging: a preliminary analysis. *J. Cereb. Blood Flow Metab.* **16,** 53–59 (1996).
3. A. J. de Crespigny, M. P. Marks, D. R. Enzmann, M. E. Moseley, Navigated diffusion imaging of normal and ischemic human brain. *Magn. Reson. Med.* **33,** 720–728 (1995).
4. C. Pierpaoli, P. Jezzard, P. J. Basser, A. Barnett, G. Di Chiro, Diffusion tensor MR imaging of the human brain. *Radiology* **201,** 637–648 (1996).
5. P. J. Basser, C. Pierpaoli, Microstructural and physiological features of tissues elucidated by quantitative-diffusion-tensor MRI. *J. Magn. Reson. B* **111,** 209–219 (1996).
6. D. M. Wimberger, T. P. Roberts, A. J. Barkovich, L. M. Prayer, M. E. Moseley, J. Kucharczyk, Identification of "premyelination" by diffusion-weighted MRI. *J. Comput. Assist. Tomogr.* **19,** 28–33 (1995).
7. J. F. Dunn, S. Ding, J. A. O'Hara, K. J. Liu, E. Rhodes, J. B. Weaver, H. M. Swartz, The apparent diffusion constant measured by MRI correlates with pO_2 in a RIF-1 tumor. *Magn. Reson. Med.* **34,** 515–519 (1995).
8. M. Eis, T. Els, M. Hoehn-Berlage, K. A. Hossmann, Quantitative diffusion MR imaging of cerebral tumor and edema. *Acta Neurochir. Suppl.* **60,** 344–6 (1994).
9. J. C. Haselgrove and J. R. Moore, Correction for distortion of echo-planar images used to calculate the apparent diffusion coefficient. *Magn. Reson. Med.* **36,** 960–964 (1996).
10. C. B. Ahn, Z. H. Cho, Analysis of eddy currents in nuclear magnetic resonance imaging. *Magn. Reson. Med.* **17,** 149–163 (1991).
11. B. R. Barker, B. T. Archer, W. A. Erdman, R. M. Peshock, A MRI gradient waveform model for automated sequence calibration. *Med. Phys.* **19,** 1483–1489 (1992).
12. D. LeBihan, R. Turner, C. T. W. Moonen, J. Peckar, Imaging of diffusion and microcirculation with gradient sensitization: design, strategy, and significance. *J. Magn. Reson. Imaging* **1,** 7–28 (1991).
13. W. S. Price, P. W. Kuchel, Effect of non-rectangular gradient pulses in the Stejskal and Tanner (diffusion) pulse sequence. *J. Magn. Reson.* **94,** 133–139 (1991).
14. T. D. Trudeau, W. T. Dixon, J. Hawkins, The effect of inhomogeneous sample susceptibility on measured diffusion anisotropy using NMR imaging. *J. Magn. Reson. B* **108,** 22–30 (1995).
15. S. J. Gibbs, C. S. Johnson, Jr., A PFG NMR experiment for accurate diffusion and flow studies in the presence of eddy currents. *J. Magn. Reson.* **93,** 395–402 (1991).
16. U. Sinha, S. Sinha, High speed diffusion imaging in the presence of eddy currents. *J. Magn. Reson. Imaging* **6,** 657–666 (1996).
17. M. P. Marks, A. deCrespigny, D. Lentz, D. R. Enzmann, G. W. Albers, M. E. Moseley, Acute and chronic stroke: navigated spin-echo diffusion-weighted MR imaging. *Radiology* **199,** 403–408 (1996).
18. S. Warach, J. Gaa, B. Stiewart, F. Wielopolski, R. R. Edelman, Acute human stroke studied by whole brain echo planar diffusion-weighted magnetic resonance imaging. *Ann. Neurol.* **37,** 231–241 (1995).
19. R. A. Knight, M. O. Dereski, J. A. Helpern, R. J. Ordidge, M. Chopp, Magnetic resonance imaging assessment of evolving focal cerebral ischemia. Comparison with histopathology in rats. *Stroke* **25,** 1252–1261 (1994).
20. T. Tsukamoto, K. King, T. K. F. Foo, E. Yoshitome, Diffusion imaging with spiral scans, *in* "Proc., SMR, 2nd Annual Meeting, 1994," p. 1032.
21. A. F. Gmitro, A. L. Alexander, Use of a projection reconstruction method to decrease motion sensitivity in diffusion-weighted MRI. *Magn. Reson. Med.* **29,** 835–838 (1993).
22. S. Mori, P. C. M. van Zijl, Diffusion-weighting by the trace of the diffusion tensor in a single scan. *Magn. Reson. Med.* **33,** 41–51 (1995).
23. P. Jezzard, R. S. Balaban, Correction for geometric distortion in echo planar images from B0 field variations. *Magn. Reson. Med.* **34,** 65–73 (1995).